ACS APPLIED MATERIALS & INTERFACES

Research Article

www.acsami.org

Programming Surface Morphology of TiO_2 Hollow Spheres and Their Superhydrophilic Films

Bo Peng, Longfei Tan, Dong Chen, Xianwei Meng, and Fangqiong Tang*

Laboratory of Controllable Preparation and Application of Nanomaterials, Technical Institute of Physics and Chemistry, Chinese Academy of Sciences, Beijing, 100190, P. R. China

Supporting Information

ABSTRACT: Long-term stable superhydrophilic films without UV irradiation consisting of hierarchical raspberrylike metal-ion-doped TiO_2 hollow spheres were fabricated by a simple spinning-coat method. The hierarchical surface morphology of metal-ion-doped TiO_2 hollow spheres can be programmed from "smooth", "moderate roughness" to "roughness" by adjusting the molar ratio of Co^{2+} ions to Zn^{2+} ions. Our results show that the substitution Co^{2+} and Zn^{2+} for Ti^{4+} has effect on the phase transformation from anatase to rutile and further lead to different papillas on the surface of hollow nanospheres. And their films consisting of corresponding hollow nanospheres can be controlled from hydrophilic to superhydrophilic: 28, 7, and 0°. Therefore, our works open an avenue to design hierarchical surface morphology of nanospheres and further fabricate antifogging superhydrophilic films.

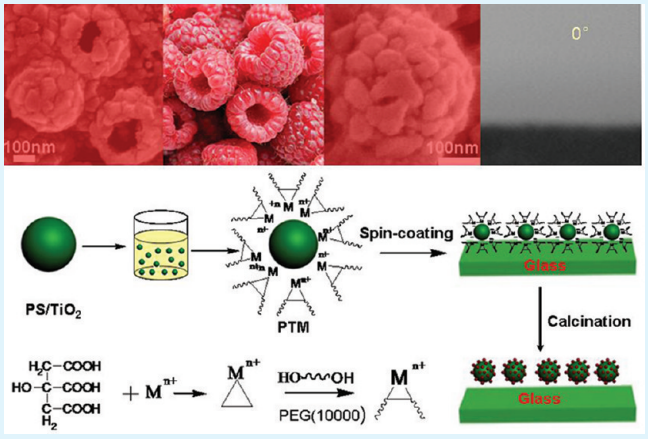

KEYWORDS: *metal-ion-doped, anatase-rutile transformation, hierarchical surface, hollow TiO_2 spheres, superhydrophilic films, without UV irradiation*

INTRODUCTION

Titania is one of the most important semiconductors that are used in many industrial applications related to photocatalysis,[1,2] sensors,[3,4] photovoltaic cells,[5,6] and pigments.[7−9] Furthermore, superhydrophobicity/superhydrophilicity on TiO_2 thin films has attract intense research interest due to their widely application in self-cleaning and antifogging.[10,11] In the past decade year, there are many reports on the formation of superhydrophilic films with TiO_2.[12−15] Feng et al. reported on the creation of superhydrophilic films consisting of inorganic nanorods fabricated from hydrophilic TiO_2 under ultraviolet (UV) irradiation.[16] Sun et al. prepared a superhydrophilic nanostrawberry TiO_2 surface by UV irradiation.[17] However, superhydrophilicity must be the photoinduced and does not be kept for a long time in the absence of UV irradiation and it restores back to hydrophobic films within minutes to hours when placed in a dark environment, which become obstructive for their numerous potential applications.[18] It is still a great challenge to fabricate superhydrophilic TiO_2 films without UV irradiation.

With the deep research of the superhydrophilic and superhydrophobic phenomena, scientists find that the excellent properties of the materials lie on their chemical compositions and surface roughness.[19−22] Recently, a few superhydrophilic TiO_2 films were prepared by increasing the film surface roughness. Hosono et al.[23] reported perpendicular TiO_2 nanosheet superhydrophilic films produced on a titanium metal sheet by hydrothermal treatment with aqueous urea. However, these films suffered from certain limitation, such as severe fabrication conditions.

Constructing hierarchical structures on the films can greatly improve their surface roughness and further enhance their wettability.[24−26] Lee et al. reported fabrication of hierarchically porous superhydrophilic thin films by LBL assembly of positively charged TiO_2 nanoparticles and negatively charged SiO_2 nanoparticles.[27] Liu et al. prepared hierarchically structured superhydrophilic surfaces consisting of self-assembling raspberrylike SiO_2 nanoparticles via LBL assembly and they further fabricated hierarchically structured porous superhydrophilic films of SiO_2 hollow spheres by combining the template method and the LBL assembly technique.[28,29] And Zorba et al. designed a hierarchical porous superhydrophilic surface consisting of random solid aggregation of small TiO_2 particles with 50 nm by sol−gel method.[30] Therefore, a promising avenue is proposed to fabricate superhydrophilic TiO_2 films without UV irradiation by programming hierarchically porous TiO_2 hollow structures as building blocks. Nevertheless, there have been few reports on programming

Received: July 29, 2011
Accepted: December 12, 2011
Published: December 12, 2011

   dx.doi.org/10.1021/am2009986 | ACS Appl. Mater. Interfaces 2012, 4, 96−101

Scheme 1. Formation of Monodisperse Hierarchical Hollow Nanospheres

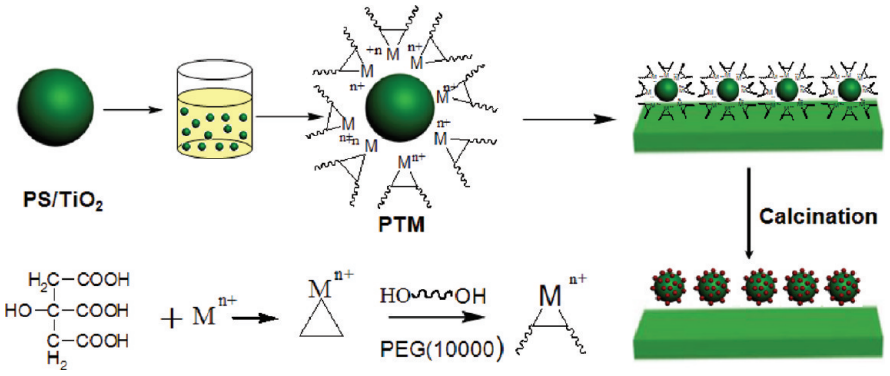

their surface morphology of building blocks to investigate the effect on the hydrophilic properties of their films so far.[31,32]

Herein, we programmed three kinds of metal-ions-doped TiO_2 hollow nanospheres with different hierarchical protruding surface morphology via a simple metal-ion-induced method, which conquer the drawbacks of the LBL methods reported, such as time-consuming and complex.[33] We further investigated the effect of their surface morphology on the wettability of films. What's more, porous superhydrophilic films consisting of hierarchical raspberrylike TiO_2 hollow spheres were fabricated by spin-coating method, which can be retained for a long time in the absence of UV irradiation. After storing in a Petri dish for more than 30 days, the superhydrophilic properties still remain obviously, suggesting that the films are suitable for antifogging purpose. In our previous work, we constructed multifunctional hollow TiO_2 spheres by using Co^{2+} ions and Zn^{2+} ions as the dopant and polystyrene particles as templates.[34] Herein, we further controlled the interesting hierarchical protruding surface morphology of hollow particles from "smooth", "moderate roughness" to "roughness", by adjusting the ratio of Co^{2+} ions to Zn^{2+} ions. We suggest that the Co^{2+} ions and Zn^{2+} ions dopant have great effect on the transformation from anatase to rutile and further influence the surface morphology of hollow spheres. The contact angle of films consisting of different corresponding hierarchical TiO_2 hollow spheres are 28°, 7°and 0°, respectively. As the surface roughness of hollow spheres is increased, the hydrophilicity of corresponding films is enhanced. Therefore, our works open a new avenue to design hierarchical surface morphology of nanospheres and further fabricate self-cleaning and antifogging superhydrophilic films.

EXPERIMENTAL DETAILS

Chemicals. Tetra-n-butyl titanate (TBT) and acetonitrile were purchased from Sigma and used without further purification. Potassium persulfate (KPS), $CoCl_2{\cdot}6H_2O$, $Zn(Ac)_2{\cdot}2H_2O$, polyethylene glycol (PEG 10000), styrene, ethanol, and ammonia were all supplied by the Beijing Chemical Reagent Company. Styrene was purified by distillation under reduced pressure. Ethanol was dehydrated by molecule sieves.

Fabrication of the PS/TiO_2 Hybrid Particles. Highly monodisperse PS/TiO_2 nanospheres were prepared by mixed-solvent method as described in our previous report:[35] 0.2 mg/mL PS spheres was dispersed in the mixed solvent of ethanol/acetonitrile (3/1 v/v) and then mixed with 0.3 mL of ammonia. Finally, the mixed solvent of ethanol/acetonitrile (3/1 v/v) containing 0.65 mL of TBT was added to the above suspension under stirring. After reacting for 1 h, the obtained particles were cleaned by three cycles of centrifugation and then dispersed in ethanol.

Preparation of Metal-Ion-Doped Particles. The monodisperse metal-ion-doped TiO_2 nanospheres were prepared by using the Pechini sol–gel process.[9,36] 0.9 mmol of $CoCl_2{\cdot}6H_2O$ and 0.3 mmol of $Zn(Ac)_2{\cdot}2H_2O$ were first dissolved in a 88 mL of water–ethanol (1/7 v/v) solution containing citric acid which was two times as much as the metal ions. The molar ratio of Co^{2+} ions to Zn^{2+} ions is tuned to be 2:1, 3:1, and 4:1. And then 4.88 g of the PEG (10000) was added. After 2 h, the 0.04 g of PS/TiO_2 hybrid spheres were added. After stirring for another 4 h, the metal-ions-coated PS/TiO_2 (MICPT) spheres were separated by centrifugation. Finally, they were annealed at 500 °C for 4 h with a heating rate of 5 °C/min and then 600 °C for 2 h with a heating rate of 2 °C/min. Metal-ion-doped TiO_2 hollow nanospheres were obtained.

Fabrication of the Hydrophilic Films. The obtained MICPT were redispersed in a water–ethanol solution (2%-5%, weight, %) and then the suspension was applied to glass substrates using a spin-coating method (KW-4A Spin Coater, Institute of Microelectronics of Chinese Academy of Sciences, 1000 rpm, 20s). Glass substrates were treated with Piranha solution (98 wt % H_2SO_4/30 wt % H_2O_2, 7/3, v/v. caution: the Pirhana solution is highly dangerous and must be used with great care) and washed with deionized water. Finally, they were annealed at 500 °C for 4 h with a heating rate of 5 °C/min and then 600 °C for 2 h with a heating rate of 2 °C/min.

CHARACTERIZATION

X-ray powder diffraction (XRD) measurement was employed D8 Focus (Germany,Bruker) γA X-ray diffractometer equipped with graphite monochromatized Cu Kα radiation (λ = 1.54 Å). A scanning electron microscope (SEM, Hitachi 4300) coupled with an energy-dispersive X-ray (EDX) spectrometer operated at 10 kV and 15 kV was used to check the morphology and elemental composition of hollow TiO_2 nanospheres. Contact angle was measured on a Phoenix 300 contact-angle system (Korea) at ambient temperature.

RESULTS AND DISCUSSION

As illustrated in Scheme 1, the highly monodisperse PS/TiO_2 nanospheres were first prepared in the mixed solvent of ethanol and acetonitrile by hydrolyzing Tetra-n-butyl titanate in the presence of ammonia, as described in our previous report.[8,35] And then, the PS/TiO_2 nanospheres were added into a water–ethanol solution containing a certain rate of $CoCl_2{\cdot}6H_2O$, $Zn(Ac)_2{\cdot}2H_2O$, citric acid, and a certain amount of polyethylene glycol (PEG), in which chelate complex of metal-ions with citric acid reacted with PEG to form polyesters. Thereby, PS/TiO_2 nanospheres were coated by polyesters and metal ions were also absorbed on the surface of PS/TiO_2 nanospheres. The MICPT were spin-coated on glass substrates. After calcinations, hydrophilic films consisting of hierarchical hollow TiO_2 nanostructures were formed.

dx.doi.org/10.1021/am2009986 | ACS Appl. Mater. Interfaces 2012, 4, 96–101

Figure 1A shows the SEM images of porous films consisting of hierarchical hollow TiO_2 spheres when the molar ratio of

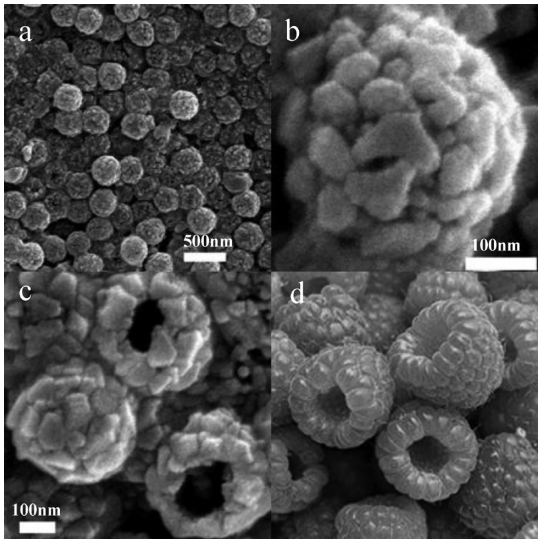

Figure 1. (a–c) SEM images of the monodisperse raspberrylike hollow TiO_2 nanospheres at different magnification. (b) Detail structures and (c) vivid hollow structures. (d) Photo image of the raspberry in nature.

Co^{2+} ions to Zn^{2+} ions is 3:1. Hollow TiO_2 spheres with diameter of about 340 nm are stacked together and there are lots of interstitial voids between hollow TiO_2 spheres. Figure 1B shows the detail information of the outer surfaces of the hollow TiO_2 spheres at a higher magnification. It clearly shows the spherical particles have papilla surfaces and the surfaces of the spheres are coated with small irregular and nonuniform particles, which results in the rough surface and typical hierarchical structures. As shown in Figure 1C, the presence of the crevasse suggests that the hollow nanostructures are formed. Furthermore, it is very vivid that shells are comprised of the aggregated small particles, which resemble the morphology of the raspberry shown in Figure 1D.[37]

We demonstrate that the protruding morphology of the hierarchical hollow TiO_2 spheres can be conveniently controlled by adjusting the ratio of Co^{2+} ions to Zn^{2+} ions. Figure 2 shows the SEM images of the obtained hollow TiO_2

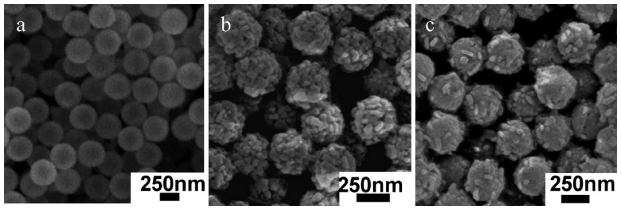

Figure 2. SEM images of the hollow nanospheres obtained at different molar ratios of Co^{2+} ions to Zn^{2+} ions: (a) 2:1, (b) 3:1,(c) 4:1.

sphere powder samples at different molar ratio of Co^{2+} ions to Zn^{2+} ions. In Figure 2A, it is clearly shown that the surface of the hollow TiO_2 spheres prepared at the ratio of 2:1 is smooth and there is no any papilla on the surface, and the shell is compact. When the ratio is increased to 3:1, the abundant protuberant small particles appear on the surface and the shells consist of many small particles, which result in the formation of hierarchical raspberry-like architectures and rough surfaces (shown in Figure 2B). It is a surprise that when the molar ratio of Co^{2+} ions to Zn^{2+} ions is increased to 4:1, the papillas decrease sharply. Although the SEM picture in Figure 2C suggests that some papillas are present, the surfaces that are not covered by small particles are predominant and fairly smooth. The typical XRD patterns of the corresponding hollow TiO_2 sphere powder samples obtained at different molar ratio of Co^{2+} ions to Zn^{2+} ions are shown in Figure 3. The strong

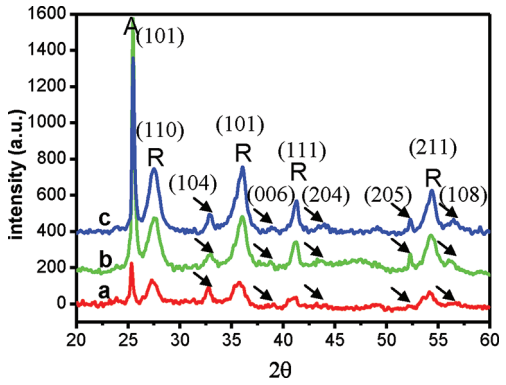

Figure 3. Corresponding XRD patterns of the hollow nanospheres (a) 2:1, (b) 3:1, (c) 4:1.

characteristic peaks corresponding to around 25.3° can be assigned to (101) plane of anatase phase (JCPDS 84–1285) and the peaks corresponding to 27.3, 35.9, 41.1, and 54.1° are in good agreement with (110), (101), (111) and (211) planes of the rutile (JCPDS 77–0443). It is noteworthy that the peak corresponding to 32.8° (signed by arrows) is assigned to (104) planes of $CoTiO_3$ (JCPDS 77–1373) and the peaks corresponding to around 38.9, 49, 52.3, and 56.5° (signed by arrows) are in good agreement with (006), (204), (205), and (108) planes of $ZnTiO_3$ (JCPDS 14–0033), which is due to high concentration of metal ion dopants.[38] Interestingly, it is found that the metal ion dopant result in the peak of (101) plane of anatase phase is shifted to higher 2θ angle as the molar ratio of Co^{2+} ions to Zn^{2+} ions is increased from 2:1 to 3:1 and 4:1. We calculated the mass fraction of the anatase phase in different samples, X_A, which is determined from the relative XRD intensities corresponding to anatase (101) and rutile (110) reflections.[39,4041]

$$X_A = 1 - [1 + 0.79(I_A/I_R)]^{-1} \quad (1)$$

where I_A and I_R is integrated intensities of anatase (101) and rutile (110) peak in XRD data, respectively. I_A/I_R is their ratio of integrated intensities. We can find that when the ratio is 2:1, the rutile phase is the predominant species and the fraction of anatase is about 48%. And when the ratio is increased to 3:1 and 4:1, the anatase phase becomes dominant, which is about 62%, 54% for 3:1 and 4:1, respectively. But all of the detectable peaks of TiO_2 hollow particles without any dopant obtained under the same conditions can be indexed as the TiO_2 with anatase structure and no peak of rutile structure is detected (see the Supporting Information, SI-1). These results indicate that the Co^{2+} and Zn^{2+} ions substitute for Ti^{4+} and influence the phase transformation from anatase to rutile. And the transformation degree depends on the molar ratio of Co^{2+} ions to Zn^{2+} ions under the same experiment conditions.[34,42] It is very interesting that the mass fraction of anatase at the ratio of 3:1 is

bigger than that of other two samples. Meanwhile, there are the most papillas on their surfaces, which result in the roughest surfaces in all samples. The average crystal size of the sample has been estimated by Scherrer's formula. The primary crystallite size calculated from (101) peak of XRD pattern (anatase) is about 40 ± 0.7, 43.7 ± 1.1, and 40.8 ± 1.5 nm, corresponding to hierarchical hollow particles obtained when the ratio of Co^{2+} ions to Zn^{2+} ions is 2/1, 3/1, 4/1, respectively. The crystallite size of sample obtained at the ratio of 3:1 is larger than that of other two samples. It is also found that the crystal size of pure TiO_2 hollow particles with anatase structure is 26.9 ± 0.2 nm, much smaller than that of metal-ion-doped TiO_2 hollow particles. Therefore, we suggest that bigger TiO_2 crystallites result in more papillas on the surface than others and the roughest surface.

Previous studies have reported that the anatase pseudoclose-packed planes of oxygen {112} were retained as the rutile close-packed planes{100} during the anatase−rutile transformation and a cooperative rearrangement of the titanium and oxygen ions occurred within this configuration, which result in an overall shrinking of the oxygen structure. Therefore, the removal of oxygen ions might be expected to accelerate the transformation.[43] For Co^{2+}/Zn^{2+}-ion-doped TiO_2, the effective ion radii of Co^{2+} ions and Zn^{2+} ions is 0.745 and 0.74 Å, respectively, which is larger than radii of Ti^{4+} (0.65 Å) and smaller than that of O^{2-} (140 Å).[44] Therefore, Co^{2+} and Zn^{2+} can be introduced into titania to substitute Ti^{4+}, leading to the formation of oxygen vacancy due to their own stoichiometry, which provide the extra space required for anatase−rutile transformation. Meanwhile, deformations of the lattice structure are produced and the deformation energy has to be released by the transformation. Therefore, the substitution of Co^{2+} and Zn^{2+} for Ti^{4+} accelerate the transformation from anatase to rutile. Because the radii of Co^{2+} and Zn^{2+} ions is very close and their ion charge is same, therefore the anatase−rutile phase transition temperature is very close and their effect on the transformation is comparable.[40] Therefore, less Co^{2+} and Zn^{2+} ions are doped into titania, less oxygen vacancies are formed, more slowly anatase transfer to rutile, which result in bigger primary crystallite and larger fraction of anatase. The elemental compositions of metal-ion-doped TiO_2 hollow spheres were verified by the energy-dispersive X-ray (EDX) spectra (see the Supporting Information, SI-2). O, Ti, Zn, and Co peaks are observed, which indicates that metal ions are doped into TiO_2 particles. The atomic ratio of Co^{2+} ions to Zn^{2+} ions is 2.03, 3.03, and 3.45 for 2/1, 3/1 and 4/1, respectively, which is comparable to the ratio of original ion source. The molar ratio of metal ions ($M^{n+}/(M^{n+} + Ti^{4+})$) is 37.8, 25.7, and 27.7% in the case that Co^{2+}/Zn^{2+} is 2/1, 3/1, 4/1, respectively. From EDX data, it is concluded that fraction of anatase and crystallite size should follow the order: 3:1 > 4:1 > 2:1, which is in good agreement with the XRD data. We further checked the surface roughness of metal-ion-doped hollow particles obtained in the case that the initial ratio of Co^{2+} ions to Zn^{2+} ions is kept at 3/1 and the molar ratio of metal ions is 30.8%, 33.9%, which was checked by EDX. It is found that the surface become smoother as molar ratio of metal ions increase (see the Supporting Information, SI-3). Moreover, the surface roughness of hollow particles follows the order: 25.7% > 27.7% > 30.8% > 33.9% ≥ 37.8%. We also investigated surface roughness of Cr^{2+}, Fe^{3+}, Al^{3+}, and Co^{2+} doped hollow particles. The molar ratio of metal ions is 24.3, 26, 33.9, 22%, respectively. And the surfaces of all of samples are smooth (see the Supporting Information, SI-4 and 5), although the molar ratio of Co^{2+} and Cr^{2+} is smaller than 25.7%. Therefore, these results show that different ions have different effect on the phase transformation from anatase to rutile. So, we believe that only when both doped metal ions and molar ratio of metal ions are right, can hollow particle with hierarchical papilla structures be obtained. Thereby, we suggest that the Co^{2+} ions and Zn^{2+} ions dopant greatly influence the phase transformation from anatase to rutile and growth rate of TiO_2 crystallization and further determine the surface morphology of the hollow metal-ion-doped TiO_2 nanospheres.

We spin-coated the Co^{2+}/Zn^{2+} modified PS/TiO_2 spheres on glass substrate and then annealed them to fabricate hydrophilic films. Figure 4 shows the SEM images of films. It is found that

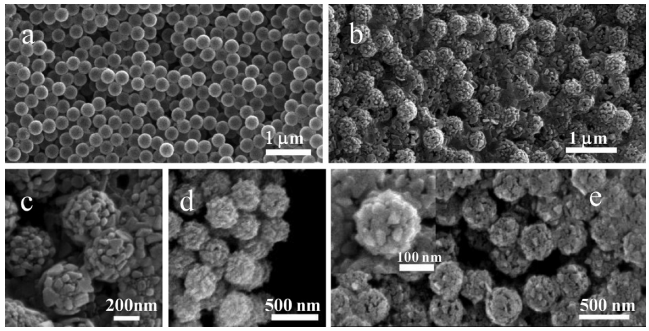

Figure 4. SEM images of films consisting of Co^{2+}/Zn^{2+}-doped hollow TiO_2 spheres: (a) Co^{2+}/Zn^{2+} = 2:1, (b) low-magnification images (Co^{2+}/Zn^{2+} = 3:1), (c) detail structures (Co^{2+}/Zn^{2+} =3:1), (d) detail structures at the edge when Co^{2+}/Zn^{2+} = 3:1, (e) Co^{2+}/Zn^{2+} = 4:1, the inset in e is the high-magnification SEM image of e.

the films at Co^{2+}/Zn^{2+} = 3:1 are much rougher than that at Co^{2+}/Zn^{2+} =2:1 and 4:1. Films at Co^{2+}/Zn^{2+} = 2:1 consist of hollow spheres with smooth surface (Figure 4a) and films at Co^{2+}/Zn^{2+} = 4:1 are made of hollow spheres with a few papillas on their surface (Figure 4e). The inset in Figure 4e shows the detail papillas structures. Figure 4b shows the surface morphology of films at Co^{2+}/Zn^{2+} = 3:1, which are porous and rough. And the surfaces of hollow Co^{2+}/Zn^{2+}-doped TiO_2 spheres show abundant protuberant particles (Figure 4c). These results are in agreement with Figure 2b. The edge image of films (Figure 4d) shows that they consist of about 3−5 layers of hollow spheres, which indicates that film's thickness is between 0.8 and 1.7 μm. The wettability of films were evaluated using a water contact meter. The immediate average contact angle (CA) on glass substrate is about 38°, shown in Figure 5a. The advancing CA of films at Co^{2+}/Zn^{2+} = 2:1 is 28°(Figure 5b), which is comparable to that of polycrystalline TiO_2 film (27.2°),[45] indicating that hollow Co^{2+}/Zn^{2+}-doped TiO_2 spheres improve the wettability. In a sharp contrast, when the ratio of Co^{2+} ions to Zn^{2+} ions is 3:1, the CA becomes 0°, showing that the obtained films have obvious superhydrophilic properties (Figure 5c). But when the ratio is increased to 4:1, the CA is 7° (Figure 5d), which is close to that of polycrystalline TiO_2 film after UV irradiation.[45] From Figures 2 and 4, we know that the surface roughness of Co^{2+}/Zn^{2+} doped TiO_2 nanospheres and films consisting of corresponding hollow spheres follows the order: 3:1 > 4:1 > 2:1 (the ratio of Co^{2+} ions to Zn^{2+} ions), which is in accordance with the wettability of films. Therefore, the increase of surface roughness can improve the wettability of films. After storing in a Petri dish

dx.doi.org/10.1021/am2009986 | ACS Appl. Mater. Interfaces 2012, 4, 96−101

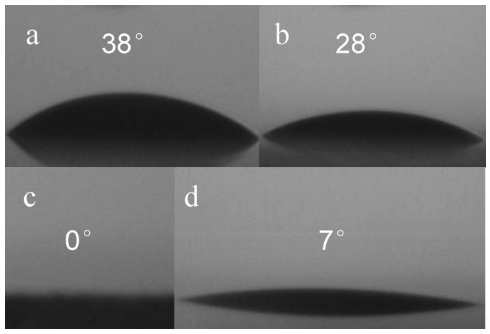

Figure 5. Photographs of water droplet shape on different films: (a) glass substrates, (b) hollow nanospheres coating (Co^{2+}/Zn^{2+} = 2:1), (c) raspberrylike hollow nanospheres coating (Co^{2+}/Zn^{2+} = 3:1) (d) hollow nanospheres coating (Co^{2+}/Zn^{2+} = 4:1).

for more than 30 days, the identical CA is observed obviously. Therefore, the superhydrophilic films show long-term stability of superhydrophilicity, which is very desirable for applications. It is well-known that the wettability of a solid surface is mainly governed by chemical composition and surface topography and increase of surface roughness can improve their wettability.[46,47] In our experiments, all conditions are same except the ratio of Co^{2+} ions to Zn^{2+} ions. So the chemical composition of hierarchically porous films composed of hollow TiO_2 is similar, which can be confirmed by XRD data. Therefore, surface topography is one of dominant factors for the intensified wettability. Hollow spheres made of films can not only result in rough morphology of films, but also nano/micropores which can be used as nanochannel to spread water. Therefore, the unexpected superhydrophilicity of the hollow-sphere films could be attributed to its characteristic nanostructure with both high surface roughness and high surface porosity.[29,31] The nanoscale capillary effect due to high surface porosity facilitates water spreading on the topmost surface at first. And then the nanoscale surface roughness of films pulls water to transport through nanopores between hollow spheres and in their shells, and further initiate 3D liquid flow and invasion through nano/micropores in 3D direction, which leads to superhydrophilicity with water entirely. Bico et al. have emphatically investigated the wetting of the superhydrophilic films with porous materials. After a drop of water is deposited on porous films, a small amount of liquid is sucked into the voids, and the remaining drop sets on a patchwork of solid and liquid. If the imbibition front progress by a quantity dx toward, the corresponding change in interfacial energy writes per unit length, dF:

$$\frac{dF}{dx} = (\gamma_{SL} - \gamma_{SV})(r - \Phi_S) + \gamma(1 - \Phi_S) \quad (2)$$

where γ_{SL}, γ_{SV}, and γ are surface tension of solid/liquid, solid/vapor, and liquid/vapor, respectively. Φ_S stands for the solid fraction remaining dry, $(r - \Phi_S)$ is the wetted area fraction, and r is the surface roughness factor, which is defined as the ratio of the actual surface area to the projected area. When dF is negative, hemiwicking should occur. The Young contact angle on an ideal film, Θ is less than Θ_C, which can be calculated from the equation[29,48]

$$\cos\Theta_C = \frac{1 - \Phi_S}{r - \Phi_S} \quad (3)$$

where Θ_C is the critical contact angle. For the porous films consisting of raspberry-like hollow nanoparticles (Co^{2+}/Zn^{2+} = 3:1), r is close unlimitedly to infinity. Therefore, Θ_C would be nearly $\pi/2$. The contact angle of water on a planar and polycrystalline TiO_2 surface is reported to be 50−70°[27,49] and 27.2°, respectively, which is less than 90°. Therefore, water can spontaneously invade into the interstitial voids between hollow TiO_2 spheres and the intrinsic hollow structure of the raspberry-like nanospheres, leading to the immediate spreading of water droplets as soon as they contacted the surface. Therefore, the hierarchical roughness and the nanoporous character of the raspberry-like hollow TiO_2 nanospheres coating establish ideal conditions for the superhydrophilicity. And for rough surface ($r > 1$, but not infinity), the critical angle can vary from 0 to 90°. And the Wenzel effect takes place. The apparent contact angle Θ^* can be calculated by the equation

$$\cos\Theta^* = r\cos\Theta \quad (4)$$

The solid roughness makes the solid surface more wettable. As the roughness increases, the wettability improves. Therefore, the contact angle of films consisting of hollow TiO_2 nanospheres (Co^{2+}/Zn^{2+} = 4:1) is smaller than that of the films consisting of hollow nanospheres (Co^{2+}/Zn^{2+} = 2:1).

CONCLUSION

We reported a new simple ion-induced method to prepare hollow monodisperse hierarchical TiO_2 nanospheres. Protruding morphology of the hollow spheres can be programmed by tuning the molar ratio of the Co^{2+} ions to Zn^{2+} ions. The surface roughness of different hollow spheres follows the order: 3:1 > 4:1 > 2:1. The wettability of films consisting of corresponding hollow spheres can be controlled from hydrophilic to superhydrophilic and their contact angle is 28, 7, and 0°, respectively. Our work will make great contribution to knowing the law of superhydrophilic properties of films and further designing antifogging and self-cleaning (superhydrophilic) TiO_2 films.

ASSOCIATED CONTENT

Supporting Information

Characterization details, XRD pattern of the TiO_2 hollow particles without any dopants, EDX spectra of hollow Co/Zn-doped TiO_2 spheres, ratio of Co^{2+} ions to Zn^{2+} ions is 3:1. This material is available free of charge via the Internet at http://pubs.acs.org/.

AUTHOR INFORMATION

Corresponding Author

*Phone: +86-10-82543521. Fax: +86-10-62554670 E-mail: tangfq@mail.ipc.ac.cn.

ACKNOWLEDGMENTS

The work was financially supported by the National Science Foundation of China (60907042, 60736001) and National Hi-Tech 863 Programme (2009AA03Z302).

REFERENCES

(1) Linsebigler, A. L.; Lu, G.; Yates, J. T. *Chem. Rev.* **1995**, *95*, 735−758.
(2) Asahi, R.; Morikawa, T.; Ohwaki, T.; Aoki, K.; Taga, Y. *Science* **2001**, *293*, 269−271.
(3) Kim, I.-D.; Rothschild, A.; Lee, B. H.; Kim, D. Y.; Jo, S. M.; Tuller, H. L. *Nano Lett.* **2006**, *6*, 2009−2013.
(4) Varghese, O. K.; Gong, D.; Paulose, M.; Ong, K. G.; Grimes, C. A. *Sens. Actuators, B* **2003**, *93*, 338−344.

(5) Oregan, B.; Gratzel, M. *Nature* **1991**, *353*, 737−740.
(6) Péchy, P.; Renouard, T.; Zakeeruddin, S. M.; Humphry-Baker, R.; Comte, P.; Liska, P.; Cevey, L.; Costa, E.; Shklover, V.; Spiccia, L.; Deacon, G. B.; Bignozzi, C. A.; Grätzel, M. *J. Am. Chem. Soc.* **2001**, *123*, 1613−1624.
(7) Comiskey, B.; Albert, J. D.; Yoshizawa, H.; Jacobson, J. *Nature* **1998**, *394*, 253−255.
(8) Peng, B.; Tang, F. Q.; Chen, D.; Ren, M. L.; Meng, X. W.; Ren, J. *J. Colloid Interface Sci.* **2009**, *329*, 62−66.
(9) Meng, X. W.; Tang, F. Q.; Peng, B.; Ren, J. *Nanoscale Res. Lett.* **2010**, *5*, 174−179.
(10) Zhang, X. T.; Sato, O.; Taguchi, M.; Einaga, Y.; Murakami, T.; Fujishima, A. *Chem. Mater.* **2005**, *17*, 696−700.
(11) Parkin, I. P.; Palgrave, R. G. *J. Mater. Chem.* **2005**, *15*, 1689−1695.
(12) Mills, A.; Elliott, N.; Parkin, I. P.; O'Neill, S. A.; Clark, R. J. *J. Photochem. Photobiol., A* **2002**, *151*, 171−179.
(13) Mills, A.; Hill, G.; Bhopal, S.; Parkin, I. P.; O'Neill, S. A. *J. Photochem. Photobiol., A* **2003**, *160*, 185−194.
(14) Fujishima, A.; Zhang, X. T.; Tryk, D. A. *Surf. Sci. Rep.* **2008**, *63*, 515−582.
(15) Wang, R.; Hashimoto, K.; Fujishima, A.; Chikuni, M.; Kojima, E.; Kitamura, A.; Shimohigoshi, M.; Watanabe, T. *Nature* **1997**, *388*, 431−432.
(16) Feng, X.; Zhai, J.; Jiang, L. *Angew. Chem., Int. Ed.* **2005**, *44*, 5115−5118.
(17) Sun, W. T.; Zhou, S. Y.; Chen, P.; Peng, L. M. *Chem Commun* **2008**, 603−605.
(18) Permpoon, S.; Houmard, M.; Riassetto, D.; Rapenne, L.; Berthome, G.; Baroux, B.; Joud, J. C.; Langlet, M. *Thin Solid Films* **2008**, *516*, 957−966.
(19) Gao, X. F.; Jiang, L. *Nature* **2004**, *432*, 36−36.
(20) Feng, L.; Li, S. H.; Li, Y. S.; Li, H. J.; Zhang, L. J.; Zhai, J.; Song, Y. L.; Liu, B. Q.; Jiang, L.; Zhu, D. B. *Adv. Mater.* **2002**, *14*, 1857−1860.
(21) Feng, X. J.; Jiang, L. *Adv. Mater.* **2006**, *18*, 3063−3078.
(22) Li, X. M.; Reinhoudt, D.; Crego-Calama, M. *Chem Soc Rev* **2007**, *36*, 1529−1529.
(23) Hosono, E.; Matsuda, H.; Honma, I.; Ichihara, M.; Zhou, H. *Langmuir* **2007**, *23*, 7447−7450.
(24) Tsai, H. J.; Lee, Y. L. *Langmuir* **2007**, *23*, 12687−12692.
(25) Ming, W.; Wu, D.; van Benthem, R.; de With, G. *Nano Lett* **2005**, *5*, 2298−2301.
(26) Nakata, K.; Sakai, M.; Ochiai, T.; Murakami, T.; Takagi, K.; Fujishima, A. *Langmuir* **2011**, *27*, 3275−3278.
(27) Lee, D.; Rubner, M. F.; Cohen, R. E. *Nano Lett* **2006**, *6*, 2305−2312.
(28) Liu, X. M.; He, J. H. *J. Colloid Interface Sci.* **2007**, *314*, 341−345.
(29) Liu, X. M.; Du, X.; He, J. H. *Chemphyschem* **2008**, *9*, 305−309.
(30) Zorba, V.; Chen, X. B.; Mao, S. S. *Appl. Phys. Lett.* **2010**, *96*, 093702.
(31) Wang, L.; Zhao, Y.; Wang, J.; Hong, X.; Zhai, J.; Jiang, L.; Wang, F. *Appl. Surf. Sci.* **2009**, *255*, 4944−4949.
(32) Chen, Y. F.; Wu, X. F.; Tian, Y. J.; Cui, Y. B.; Wei, L. Q.; Wang, Q. *J. Phys. Chem. C* **2007**, *111*, 9704−9708.
(33) Qian, Z.; Zhang, Z.; Song, L.; Liu, H. *J. Mater. Chem.* **2009**, *19*, 1297−1304.
(34) Peng, B.; Meng, X.; Tang, F.; Ren, X.; Chen, D.; Ren, J. *J. Phys. Chem. C* **2009**, *113*, 20240−20245.
(35) Tang, F. Q.; Wang, P.; Chen, D. *Langmuir* **2006**, *22*, 4832−4835.
(36) Lin, J.; Lin, C. K.; Li, Y. Y.; Yu, M.; Yang, P. P. *Adv. Funct. Mater.* **2007**, *17*, 1459−1465.
(37) http://en.wikipedia.org/wiki/Raspberry.
(38) Verma, K. C.; Sharma, S.; Thakur, N.; Kotnala, R. K. *J. Cryst. Growth* **2011**, *321*, 19−23.
(39) Lee, G. D.; Ryu, Y. C.; Kim, T. G.; Seo, G. S.; Park, J. H.; Suh, C. S.; Park, S. S.; Hong, S. S. *J. Ind. Eng. Chem.* **2008**, *14*, 213−218.
(40) Rodriguez, R.; Vargas, S.; Arroyo, R.; Haro, E. *J. Mater. Res.* **1999**, *14*, 3932−3937.
(41) Debnath, R.; Chaudhuri, J. *J. Mater. Res.* **1992**, *7*, 3348−3351.
(42) Ishigaki, T.; Wang, X. H.; Li, J. G.; Kamiyama, H.; Katada, M.; Ohashi, N.; Moriyoshi, Y. *J. Am. Chem. Soc.* **2005**, *127*, 10982−10990.
(43) Shannon, R. D.; Pask, J. A. *J. Am. Ceram. Soc.* **1965**, *48*, 391−398.
(44) Kim, H. T.; Lanagan, M. T. *J. Am. Ceram. Soc.* **2003**, *86*, 1874−1878.
(45) Sakai, N.; Fujishima, A.; Watanabe, T.; Hashimoto, K. *J. Phys. Chem. B* **2001**, *105*, 3023−3026.
(46) Chen, D.; Tan, L. F.; Liu, H. Y.; Tang, F. Q.; Hu, J. Y.; Li, Y. *Chemsuschem* **2010**, *3*, 1031−1035.
(47) Chen, D.; Tan, L. F.; Liu, H. Y. *Langmuir* **2010**, *26*, 4675−4679.
(48) Quere, D.; Bico, J.; Thiele, U. *Colloids Surf., A* **2002**, *206*, 41−46.
(49) Ralston, J.; Stevens, N.; Priest, C. I.; Sedev, R. *Langmuir* **2003**, *19*, 3272−3275.